

Research paper

Development of spontaneous recurrent seizures accompanied with increased rates of interictal spikes and decreased hippocampal delta and theta activities following extended kindling in mice



Hongmei Song ^{a,c}, Bryan Mah ^c, Yuqing Sun ^c, Nancy Aloysius ^c, Yang Bai ^{b,*}, Liang Zhang ^{c,d,**}

^a Department of Neurosurgery, the First Hospital of Jilin University, China

^b Department of Neuro-Oncology, the First Hospital of Jilin University, China

^c Krembil Research Institute, University Health Network, Canada

^d Division of Neurology, Department of Medicine, University of Toronto, Toronto, Ontario, Canada

ARTICLE INFO

ABSTRACT

Keywords:

Delta
EEG
Epilepsy
Epileptiform
Interictal spikes
Seizures
Theta

Interictal epileptiform discharges refer to aberrant brain electrographic signals between seizures and feature intermittent interictal spikes (ISs), sharp waves, and/or abnormal rhythms. Recognition of these epileptiform activities by electroencephalographic (EEG) examinations greatly aids epilepsy diagnosis and localization of the seizure onset zone. ISs are a major form of interictal epileptiform discharges recognized in animal models of epilepsy. Progressive changes in IS waveforms, IS rates, and/or associated fast ripple oscillations have been shown to precede the development of spontaneous recurrent seizures (SRS) in various animal models. IS expressions in the kindling model of epilepsy have been demonstrated but IS changes during the course of SRS development in extended kindled animals remain to be detailed. We hence addressed this issue using a mouse model of kindling-induced SRS. Adult C57 black mice received twice daily hippocampal stimulations until SRS occurrence, with 24-h EEG monitoring performed following 50, 80, and ≥ 100 stimulations and after observation of SRS. In the stimulated hippocampus, increases in spontaneous ISs rates, but not in IS waveforms nor IS-associated fast ripples, along with decreased frequencies of hippocampal delta and theta rhythms, were observed before SRS onset. Comparable increases in IS rates were further observed in the unstimulated hippocampus, piriform cortex, and entorhinal cortex, but not in the unstimulated parietal cortex and dorsomedial thalamus. These data provide original evidence suggesting that increases in hippocampal IS rates, together with reductions in hippocampal delta and theta rhythms are closely associated with development of SRS in a rodent kindling model.

1. Introduction

Epilepsy is a chronic neurological disorder characterized by persistent predisposition to occurrence of unprovoked seizures and cognitive/psychological comorbidity. Temporal lobe epilepsy is the most common type of epilepsy seen in adult and aging populations and has high diversity in etiology, clinical-electroencephalographic (EEG) manifestation, and comorbidity (Thom and Bertram, 2012). Interictal epileptiform discharges are intermittent EEG signals between seizures and represented by interictal spikes (ISs), sharp waves, and/or abnormal rhythms.

The incidences and expression patterns of interictal epileptiform discharges vary in individual patients depending on the type of epilepsy, disease progress, and/or brain pathology (Pillai and Sperling, 2006; Tatum et al., 2018). EEG assessments of interictal epileptiform discharges are of great values for diagnosis of epileptic conditions and for localizing the seizure onset zone (Tatum et al., 2018). However, it may be difficult to examine the influence or impact of interictal epileptiform discharges on epileptogenesis and progression in patients, as repeated EEG recordings over a chronic period are generally not suitable in clinical settings. Therefore, experimental studies in animal models of

* Correspondence to: Y. Bai, Department of Neuro-Oncology, Neurosurgery Center, the First Hospital of Jilin University, 19-319048, 3rd Building, 1 Xinmin Street, Chaoyang District, Changchun, China.

** Corresponding author at: L. Zhang, Krembil Research Institute, Toronto Western Hospital, University Health Network, 7th floor, Room 407, Krembil Discovery Tower, 60 Leonard Ave, Toronto M5T2S8, Ontario, Canada.

E-mail addresses: songhm@jlu.edu.cn (H. Song), baiyang0221@jlu.edu.cn (Y. Bai), [liang.zhang@uhn.ca](mailto.liang.zhang@uhn.ca) (L. Zhang).

epilepsy may offer relevant information.

Intraperitoneal or intracranial applications of kainic acid (a kainate glutamate receptor agonist) or pilocarpine (a muscarinic receptor agonist) are commonly used to generate rodent models of temporal lobe epilepsy (Löscher, 2017; Lévesque et al., 2021a; Lévesque et al., 2021b; Rusina et al., 2021). In these models, animals experience an acute episode of status epilepticus, then a seizure-free latent period (ranging from several days to a few weeks) and exhibit spontaneous recurrent seizures (SRS) afterwards. Spontaneous ISs are the most consistently observed signs of epileptiform activity in the latent period (Bragin et al., 2004; White et al., 2010; Chauvière et al., 2012; Salami et al., 2014; Bajorat et al., 2016; Li et al., 2018; Sheybani et al., 2018; Marchionni et al., 2019; Wang et al., 2019; Lévesque et al., 2021b; Lévesque et al., 2021a; Lévesque et al., 2021b; Drexel et al., 2022; see recent reviews by Engel Jr and Pitkänen, 2020; Lévesque et al., 2023). Several studies have characterized ISs during the latent period and until the first event of SRS via continuous intracranial EEG or local field potential (LFP) monitoring. For example, White et al. (2010) have shown that increases in IS rates and IS clusters were strongly correlated with SRS development in a rat kainate model. A study by Chauvière et al. (2012) distinguished two types of hippocampal ISs, i.e., type 1 and type 2, defined respectively by presence or absence of a post-spike wave, in rats with pilocarpine- or kainate-induced SRS. The number, amplitude, and duration of type 1 ISs started to decrease, whereas the number of type 2 ISs increased, several days before the first detected SRS. Fast ripples (FRs) with oscillatory activities of 250–500 Hz are considered an electrographic biomarker of epilepsy (reviewed by Engel Jr and Pitkänen, 2020; Lévesque et al., 2023; Lévesque et al., 2021a, 2021b) have demonstrated that FRs precede SRS occurrence in a mouse pilocarpine model, with greatly increased coherent expression of FR and type 1 ISs observed in the late versus the early and middle phases of the latent period. The above studies would thus indicate that progressive changes in IS patterns during the latent period are a predictive marker of SRS occurrence.

Kindling, in reference to the development of epileptiform activity and seizures elicited by brief and repeated electrical stimulation of a limbic structure, has long been used to model temporal lobe epilepsy in animals (Gorter et al., 2016; Sutula and Kotloski, 2017). While kindling via the classic protocol (lasting a few weeks) does not generally induce SRS, extended kindling (over a few months) is able to induce SRS in several animal species, including monkeys (Wada and Osawa, 1976), dogs (Wauquier et al., 1979; Shouse et al., 1990), cats (Wada et al., 1974; Gotman, 1984; Gotman, 1984; Gigli and Gotman, 1991; Hiyoshi et al., 1993), rats (Pinel and Rovner, 1978a, 1978b; Milgram et al., 1995; Michalakis et al., 1998; Sayin et al., 2003; Brandt et al., 2004), and mice (Song et al., 2018; Liu et al., 2021). Spontaneous ISs have been observed in extended kindled animals (Wada and Osawa, 1976; Pinel and Rovner, 1978b; Gotman, 1984; Gigli and Gotman, 1991; Brandt et al., 2004; Song et al., 2018). In extended kindled cats, IS rates were found to be either decreased or increased following an evoked seizure or an SRS event, and the changes in IS rates did not appear to be related to the probability of SRS occurrence (Gotman, 1984; Gigli and Gotman, 1991). The waveforms, types, and incidences of ISs have been demonstrated in rats that exhibited SRS following extended kindling (Pinel and Rovner, 1978a, 1978b; Milgram et al., 1995; Michalakis et al., 1998; Sayin et al., 2003; Brandt et al., 2004). Overall, however, IS changes during extended kindling and upon SRS development have not been detailed. We thus aim to provide information in this respect by examining ISs in a mouse model of extended hippocampal kindling (Song et al., 2018; Liu et al., 2019, 2021; Zahra et al., 2022). Specifically, we question whether progressive changes occur towards SRS development in IS waveforms, IS rates, and associated FRs.

2. Methods

2.1. Animals

C57 black mice (C57BL/6 N, male, Charles River Laboratory, Saint-Constant, Quebec, Canada) were housed under standard cage conditions and maintained at 22–23 °C with a 12-h light on/off cycle (light-on starting at 6:00 AM). Kindling was induced in middle-aged mice (11–13 months old) (Flurkey et al., 2007) to model new-onset cases of temporal lobe epilepsy occurring in adult and aging populations (Ferlazzo et al., 2016). All experimentations described below were reviewed and approved by the Animal Care Committee of the University Health Network and were in accordance with the Guidelines of the Canadian Council on Animal Care.

2.2. Electrode implantation, hippocampal kindling, and LFP monitoring

Electrode implantation, LFP recordings, and hippocampal kindling were performed as previously described (Wu et al., 2008; Bin et al., 2017; Song et al., 2018; Liu et al., 2021). All electrodes were made of polyamide-insulated stainless-steel wires (110 µm outer diameter; Plastics One, Roanoke, Virginia, USA). Two pairs of twisted-wire bipolar electrodes were implanted in each mouse. The first electrode pair was aimed at the hippocampal CA3 region (bregma –2.5 mm, lateral 3.0 mm, depth 3.0 mm; Franklin and Paxinos, 1997) to deliver kindling stimulation and obtain LFP recordings. The second electrode pair was positioned to target one of five non-stimulated forebrain structures: contralateral hippocampal CA3, ipsilateral or contralateral parietal cortex (bregma –0.5 mm, lateral 2.0 mm, depth 0.5 mm), ipsilateral piriform cortex (bregma 0.5 mm, lateral 3.0 mm, depth 5.0 mm), ipsilateral entorhinal cortex (bregma –3.5 mm, lateral 4.0 mm, depth 5.0 mm), and contralateral dorsomedial thalamus (bregma –1.5 mm, lateral 0.5 mm, depth 3.5 mm). These non-stimulated structures were selected according to previous studies in extended kindled monkeys and cats (Wada et al., 1974; Wada and Osawa, 1976; Gotman, 1984; Gigli and Gotman, 1991; Hiyoshi et al., 1993). We used this implantation approach to assess regional LFP signals while minimizing potential complications of multi-electrode implantations in the small mouse brain. Throughout the text, the five groups are referred to as hippocampal-hippocampal, hippocampal-cortical, hippocampal-piriform, hippocampal-entorhinal, and hippocampal-thalamic, respectively. A reference electrode was positioned in the frontal area (bregma +1.5 mm, lateral 1.0 mm, depth 0.5 mm). Electrode tip locations were verified by histology after completion of experiments (Liu et al., 2021; Supplementary Fig. 1).

A train of stimuli (pulse width 0.5 ms, 60 Hz for 2 s) was used for hippocampal kindling stimulation. An ascending series of stimulations was performed before kindling to determine the threshold of evoked after-discharges in individual mice. The initial threshold values were in a range of 20–85 µA. Subsequent kindling stimulations at 25% above the initial threshold value were applied twice daily until ≥2 SRS events per day were detected (see below). Control mice received similar electrode implantation procedures and were subjected to twice-daily handling manipulations for 60 days.

Differential LFP recordings were made through the twisted-wire bipolar electrodes. Signals were collected by microelectrode AC amplifiers (model 1800 or 3000, AM Systems; Sequim, Washington, USA), with an input frequency band of 0.1–1000 Hz and an amplification gain of 1000 or 3000. Amplifier output signals were digitized at 5000 or 10,000 Hz (Digidata 1440 A or 1550, Molecular Devices; Sunnyvale, CA, USA). Data acquisition, storage and analyses were done using pClamp software (Version 10; Molecular Devices).

Continuous LFP-video monitoring was performed in free-moving mice. For control mice, 24-h LFP-video monitoring was made before (baseline) and after 60 days of handling manipulations. For kindled mice, 24-h monitoring was performed before (baseline) and following

50, 80, 100, 120, or 140 stimulations. If ≥ 2 SRS events were detected in the 24-h monitoring period, kindling stimulation was terminated, and LFP-video monitoring was continued for up to 7 consecutive days to assess SRS in the early post-kindling phase (early SRS). If suitable, continuous LFP-video monitoring for up to 7 consecutive days per session was performed 6–12 weeks later to assess SRS in the late post-kindling phase (late SRS; Fig. 1A).

2.3. Data analysis

Data obtained from individual mice were visually inspected by experimenters and then selected for analysis. SRS were recognized by occurrences of spontaneous discharges and associated convulsions. Discharges were defined by repetitive spike waveforms with amplitudes approximately 2 times the background signal level and durations ≥ 10 s (Song et al., 2018; Liu et al., 2021). A modified Racine scale for mice was used to evaluate convulsive severity (Racine, 1972; Reddy and Rogawski, 2010; Reddy and Mohan, 2011; Zahra et al., 2022).

2.3.1. Selection of LFP data segments

LFP signal segments with dominant activity in delta (0.1–4 Hz) or theta (5–12 Hz) frequency bands (see below) and without evident artifacts were selected for IS analysis. The delta segments were collected in periods where mice were sleep or in stable immobility, and were each 10 min long (Chauvière et al., 2012; Salami et al., 2014; Lévesque et al., 2015). The theta segments were selected from periods where the mice were awake but largely immobile and were each 0.5–3 min long. Multiple theta segments with a cumulative length of 5–12 min were collected from individual mice at different experimental times. Because the appearance of hippocampal theta activity was not as steady as delta activity, theta segments of variable lengths were collected to analyze theta signals in relatively isolation. The delta and theta segments were selected before kindling (baseline monitoring), following 50, 80, and 100–140 stimulations without SRS detected in a 24-h monitoring period, and after observations of early and late SRS. Overall, while hippocampal IS signals were suppressed for a few min following each SRS event, ISs that occurred subsequently prior to next SRS event were relatively stable in their incidences. To minimize post-ictal influences on IS activity and to analyze relatively artefact-free LFP signals, the delta and theta segments were selected after an interval of 1–6 h following an event of SRS or evoked seizures.

2.3.2. Power spectrum analysis

Spectral plots (rectangular function, 0.15 Hz spectral resolution, averaged with 50% window overlap) were generated using Clampfit software (Molecular Devices). Signals in a frequency band of 0.1–4 Hz or 5–12 Hz were considered as delta or theta activity respectively. For assessing delta activity, spectral plots were generated from 10-min delta segments and peak delta frequency and corresponding powers were measured from the plots. Delta activity dominance was recognized if the power of peak delta frequency was ≥ 2 -fold (linear scale) that of 8 Hz signals in the same plots. For assessing theta activity, spectral plots were generated from individual theta segments, and theta activity dominance was considered if the power of peak theta frequency was ≥ 2 -fold (linear scale) that of 4 Hz signals. Spectral plots of 3–6 theta segments were averaged, and peak theta frequency and corresponding power were measured from averaged plots.

2.3.3. Detection of ISs and “baseline” spikes

ISs were detected using a threshold crossing approach (Chauvière et al., 2012; Salami et al., 2014; Lévesque et al., 2015). Specifically, standard deviation (SD) values of background LFP signals were calculated from selected data segments. Spike waveforms were searched via a sliding time window of 300 ms, applying threshold-based event detection functions of Clampfit software (El-Hayek et al., 2013; Song et al., 2018) (Fig. 1B-E). For ISs that displayed biphasic waveforms (Fig. 1D-E)

or separate upward and downward waveforms, the waveforms with larger amplitudes and more frequent expression were analyzed. The threshold for triggering spike detection was set at 4 SD of the mean value of background signals (Chauvière et al., 2012; Salami et al., 2014; Lévesque et al., 2015), except for analysis of regional IS coherence. In the latter, the threshold for triggering spike detection was set at 6 SD of the mean value of background signals, as to minimize complications related to ISs with multiple peaks (see below). A period of 100 ms was set to determine the mean amplitude of pre-spike background signals, and spike peak was determined in the next 100 ms. The spike's falling phase was assessed over a period of 200 ms, with a detection threshold set at 2 SD of the mean background signals. Individual spike waveforms were recognized as such if they had amplitudes ≥ 4 SD from the mean background signals and their falling phases returned to ≤ 2 SD from mean background levels within 200 ms. We used these settings to detect ISs with multiple peaks that were above the spike detection threshold (Fig. 1C-E). All detected ISs were visually inspected, and false events were rejected.

“Baseline” spontaneous spikes were similarly analyzed as described above. Assessed in the delta segments of the control mice ($n = 10$), hippocampal spikes were 27.8 ± 8.2 events/10 min before and 44.3 ± 9.8 events/10 min following the handling manipulation. There was no significant difference in these two measures (paired *t*-test, $t = -1.17$, $df = 9$, $p = 0.273$). Measured in the delta segments sampled before hippocampal kindling, the rates of spontaneous hippocampal spikes were 40.9 ± 7.8 events/10 min ($n = 41$ mice), which were like the control measures but significantly lower than those obtained following hippocampal kindling (see Results). Overall, these “baseline” hippocampal spikes were dominated by simple or mono-phasic morphologies (see Results for details), and their amplitudes were greater than those of “physiological” hippocampal sharp waves (Buzsáki, 2015). Together these observations suggest that the chromic handling manipulation is not a causal factor of IS genesis and that local lesions or irritations resulting from electrode implantation (Blackwood et al., 1982; Löscher et al., 1995, 1999; Bankstahl et al., 2014; Tse et al., 2021) in the small mouse brain may contribute to occurrence of spontaneous spikes (see also Discussion).

2.3.4. FR detection

FRs were analyzed based on criteria established by previous studies (Bragin et al., 2004; Lévesque et al., 2012; Salami et al., 2014). To detect IS-associated FRs, IS signals detected from delta segments were treated with a band-passing filter (Bessel, 250–500 Hz). SD values of filtered signals were calculated, and the threshold-based search method mentioned above was employed to detect FRs. The threshold for triggering FR detection was set at 3 SD of the mean value of filtered background signals. An IS-associated FR event was considered if it comprised 4 or more consecutive oscillatory events that were above the FR detection threshold, with inter-event intervals ≤ 4 ms and in a time window of ± 100 ms of original IS signals.

2.4. Statistical analysis

Origin (Northampton, MA, USA) or GraphPad (Boston, MA, USA) software was used for statistical tests. Data were presented as the mean and the standard error of the mean (SEM) throughout the text and figures except where specified. Statistical significance was set at $p < 0.05$. The Shapiro-Wilk test was used to assess data normality. For assessing group differences, the Student's *t*-test or one-way ANOVA followed by Bonferroni's post-hoc test was used for normally distributed data, and the Mann-Whitney *U* test or nonparametric Kruskal-Wallis test followed by Dunn's post-hoc test was employed for non-normally distributed data.

3. Results

Data were collected from 61 mice that underwent extended

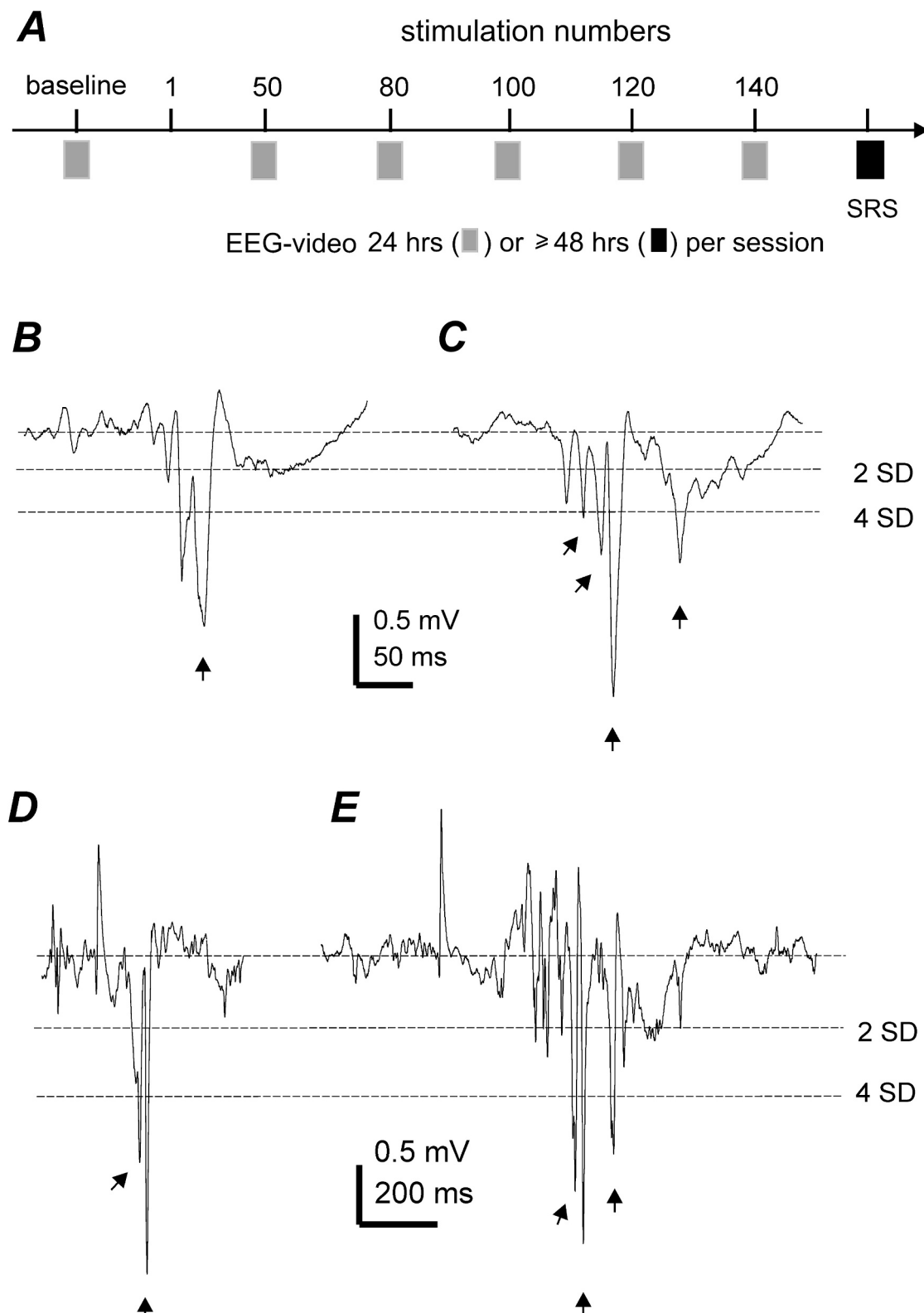


Fig. 1. LFP-video monitoring and IS detection protocols. A, 24-h LFP-video monitoring was performed before kindling (baseline) and following 50, 80, 100, 120, or 140 stimulations until ≥ 2 SRS events were detected in the 24-h monitoring period. LFP-video monitoring was additionally performed up to 7 days after termination of kindling to assess SRS in the early post-kindling phase (early SRS). Similar monitoring resumed 6–12 weeks later in some mice to assess SRS in the late post-kindling phase (late SRS). B–E, representative ISs recorded from a mouse following 80 stimulations (B–C) and after observation of late SRS (D–E). Dotted lines indicate putative baseline and 2 and 4 standard deviation (SD) levels above mean background signals. Filled arrows indicate spike waveforms with peaks above 4 SD from baseline and falling phases below the 2 SD level.

hippocampal kindling. Individual mice were under 24-h LFP-video monitoring following 50, 80, 100, 120, or 140 kindling stimulations. Kindling stimulations were terminated if ≥ 2 SRS events were detected in the 24-h monitoring period (Fig. 1A). Overall, SRS were observed following 110.2 ± 2.8 hippocampal kindling stimulations. SRS detected within 7 days and 6–12 weeks after termination of kindling are referred to early and late SRS respectively. IS data collected following 100, 120, and 140 stimulations but prior to SRS occurrence were pooled together as “ ≥ 100 stimulations” because of relatively small sizes for the latter two time points. ISs recorded from the stimulated hippocampus are referred to as hippocampal ISs, except where specified. For mice in the hippocampal-thalamic group, 24-h LFP-video monitoring during extended kindling was not performed because thalamic stimulations were repeatedly applied to test their effects on evoked seizures (manuscript to be submitted). Therefore, for this group only data collected after observation of SRS are presented further below. Hippocampal kindling was terminated in 24 mice that experienced 22–39 stimulations

due to a loss of implanted electrodes or severe skin infection. Observations from these mice are not included in data analysis.

4. Changes in waveforms of spontaneous hippocampal ISs

Previous studies have observed spontaneous ISs in animals that underwent classical kindling (Kairiss et al., 1984; Racine et al., 1988; Sobieszek, 1989; Leung, 1990, 1994; Kogure, 1997) or extended kindling (Wada and Osawa, 1976; Pinel and Rovner, 1978b; Gotman, 1984; Gigli and Gotman, 1991; Brandt et al., 2004; Song et al., 2018). These ISs were expressed in multiple forebrain structures, including the hippocampus, and displayed simple or complex waveforms. Considering that changes in type 1 and type 2 ISs preceded SRS development in rat pilocarpine or kainate models (Chauvière et al., 2012), we examined whether the waveforms of hippocampal ISs undergo progressive changes towards SRS development in our model. Hippocampal ISs with simple or complex waveforms were observed in individual mice at

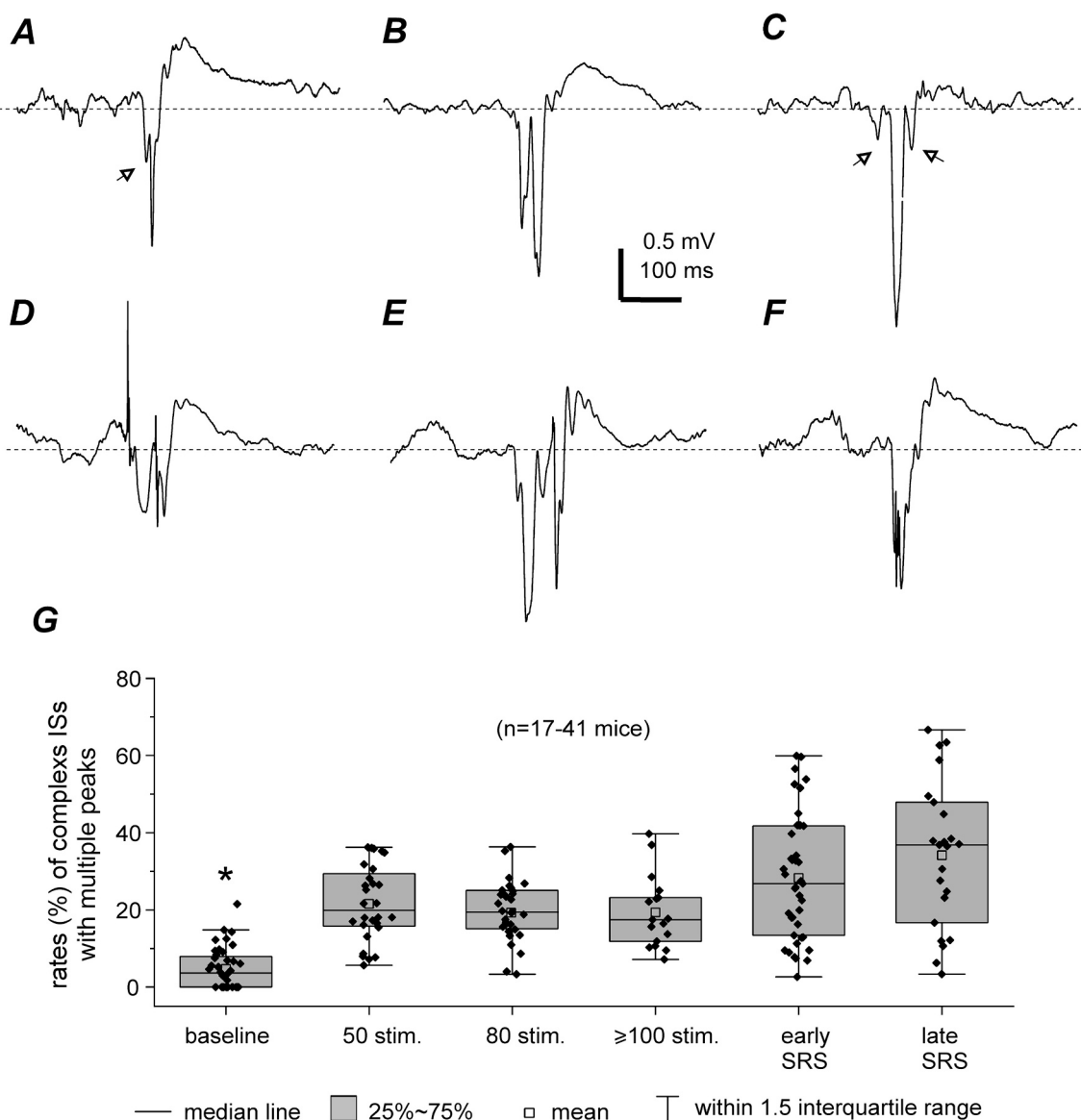


Fig. 2. Hippocampal ISs displaying simple or complex waveforms. A-F, representative hippocampal ISs sampled from a 10-min delta segment following 80 stimulations. Dotted lines denote putative baseline. Simple ISs display monophasic waveforms with (A) or without (C) a post-spike wave and small components (open arrows) in their raising and/or falling phases. Complex ISs display monophasic (B, F) or biphasic (E-F) waveforms and multiple peaks. A post-spike wave is noticeable for complex ISs in B and F. G, proportions of complex ISs with multi-peak waveforms estimated as percentiles of total ISs detected from delta segments. Data presented in box plot. *, $p < 0.05$, nonparametric Kruskal-Wallis test, baseline vs. other measures.

different time points following kindling. Simple ISs were distinguished by a monophasic waveform with or without a post-spike wave component (Fig. 2A or C), and might resemble the type 1 and type 2 ISs recognized in the rat models (Chauvière et al., 2012; Lévesque et al., 2021a; Lévesque et al., 2021b). However, these simple ISs often contained small components that superimposed onto or appeared near the rising and/or falling phase of the main spike waveform (denoted by open arrows in Fig. 2A, C). Such waveforms thus seemed to be different from those describing type 1 and type 2 ISs. In addition, complex ISs were often followed by a post-spike wave component (Fig. 2B, D and F).

Complex hippocampal ISs were monophasic (Fig. 1B, C; Fig. 2B, F) or biphasic (Fig. 1D-E; Fig. 2D) in morphology and featured multiple peaks that were above the spike detecting threshold, with inter-peak intervals of ≤ 100 ms in most cases (Fig. 1C-E; Fig. 2B, D-F). To examine the incidence of complex ISs at different time points following kindling, we estimated the rate of ISs with ≥ 3 peaks by normalizing their incidences as percentiles of the total ISs detected from delta segments. Fig. 2G presents data collected from mice in the hippocampal-hippocampal, hippocampal-cortical, hippocampal-piriform, and hippocampal-entorhinal groups ($n = 17$ –41 per group). The mean rates of the multi-peak complex ISs were respectively $21.56\% \pm 1.84\%$, $19.70\% \pm 1.37\%$, and $19.34\% \pm 2.26\%$ following 50, 80, and ≥ 100 stimulations, and $28.24\% \pm 2.53\%$ and $34.13\% \pm 3.92\%$ after observation of early and late SRS. There was no significant difference among these rates, but they were significantly greater than that of complex spikes observed before kindling ($4.67\% \pm 0.84\%$) (nonparametric Kruskal-Wallis test; Chi-square 81.1, df = 5, prob. > Chi-square < 0.0001; Dunn's test, p < or > 0.05). Together, these observations suggest that SRS development is not accompanied with progressive changes in hippocampal IS waveforms in our model. Based on these observations, we did not separate type 1- from type 2-like ISs and combined the simple and complex hippocampal ISs in following analysis.

5. Changes in hippocampal IS rates

Previous studies have reported that extended kindled animals exhibited spontaneous ISs predominantly during inactive behaviors such as sleep and stable immobility (Gotman, 1984; Pinel and Rovner, 1978a, 1978b; Brandt et al., 2004). Our previous study showed that in kindled mice that exhibited SRS, hippocampal ISs occurred not only during the inactive behaviors but also in association with hippocampal theta rhythm (Song et al., 2018). The rodent hippocampus is known to exhibit large- or small-amplitude irregular activity at ≤ 4 Hz during inactive behaviors (such as slow wave sleep or stable immobility) and theta rhythm of 5–12 Hz during active behaviors (such as exploration and movement, as well as alert immobility) (Vanderwolf, 1969; Leung et al., 1982; Jarosiewicz et al., 2002; Buzsáki, 2002, 2015; Mysin and Shubina, 2023). We therefore measured the rates of spontaneous hippocampal ISs in delta and theta EEG segments to explore behavioral state-dependent changes in IS activity.

Fig. 3A-B present representative examples of hippocampal LFP epochs collected from a single mouse at different experimental time points. No spontaneous hippocampal spiking activity was observed in this mouse before kindling (baseline monitoring). On examination following 50 and 80 stimulations, intermittent hippocampal ISs with simple or complex waveforms were evident in delta segments (Fig. 3B-D, left), whereas spontaneous IS was absent in theta segments. SRS were detected in this mouse following 100 stimulations. Examples of spontaneous discharges detected from this mouse are presented in Supplementary Fig. 2. In delta segments sampled after observation of early and late SRS, hippocampal ISs occurred more frequently and rhythmically, and displayed more complex waveforms compared to those observed before SRS occurrence. Hippocampal ISs of irregular occurrence were noticeable in theta segments sampled after observation of early and late SRS.

The rates of spontaneous hippocampal ISs were measured in mice in

the hippocampal-hippocampal, hippocampal-cortical, hippocampal-piriform, and hippocampal-entorhinal groups at different experimental time points (Fig. 3C-D). Assessed from delta segments, IS rates were respectively 201.3 ± 20.8 , 242.0 ± 30.7 , and 276.8 ± 31.7 events/10 min following 50, 80, and ≥ 100 stimulations, and 385.8 ± 33.0 and 525.7 ± 59.5 events/10 min after observation of early and late SRS. The IS rates after SRS occurrence were significantly greater than those following 50 and 80 stimulations, and all these measures were significantly increased from the baseline spike rate (40.9 ± 7.8 events/10 min) (nonparametric Kruskal-Wallis test, $n = 24$ –40 per group; Chi-square 97.9, df = 5, prob. > Chi-square < 0.0001; Dunn's test, p < 0.05; Fig. 3C). Three mice were euthanized after 147–156 stimulations due to a loss of implanted electrodes or severe skin lesion. When being monitored following 100 and 140 stimulations, these mice exhibited no SRS but frequent hippocampal ISs, with IS rates of 50–116 events/10 min and 179–395 events/10 min respectively. These measures were in the range of IS rates measured from mice with detected SRS. Together these observations suggest that the overall rates of hippocampal ISs were progressively increased following extended kindling.

Assessed from theta segments, the rates of spontaneous ISs were respectively 8.5 ± 3.0 , 4.9 ± 1.1 , and 6.5 ± 1.0 events per min following 50, 80, and ≥ 100 stimulations, and 21.6 ± 3.5 and 33.4 ± 6.7 events per min after observation of early and late SRS. Spontaneous IS rates after SRS occurrence were significantly greater than those recorded from 50, 80, and ≥ 100 stimulations, as well as the baseline spike rate (2.7 ± 0.6 events/min); however, there was no significant differences among the latter four measures (nonparametric Kruskal-Wallis test, $n = 24$ –40 per group; Chi-square 58.1, df = 5, prob. > Chi-square < 0.0001; Dunn's test, p < or > 0.05; Fig. 3D). With respect to the IS rate changes following 50, 80 and ≥ 100 stimulations, the patterns were distinct between theta and delta segments. This suggested an influence of behavioral state-dependent background activities on hippocampal IS progression.

Supplementary Table 1 presents SRS daily incidences, hippocampal discharge durations, motor seizure stages and hippocampal ISs of delta segments assessed for individual mice. To examine impacts of SRS on ISs, we plotted hippocampal IS rates against SRS daily incidences, mean durations of hippocampal discharges or mean stages of motor seizures (Fig. 3E-F). Linear regression analysis revealed a relatively strong relationship between IS rates and SRS daily incidences, hippocampal discharge durations or motor seizure stages ($R^2 = 0.70$, 0.73 or 0.70, DF = 57, 57 or 43, F = 135.2, 153.8 or 101.2; p < 0.0001). Together these and above observations suggest that increased IS activity is closely associated with SRS development and that SRS are an important influence factor of hippocampal ISs in our kindling model.

6. Changes in IS-associated hippocampal delta and theta activities

To examine whether IS occurrence was associated with changes in hippocampal delta and theta activity, spectral plots were generated from corresponding data segments in which hippocampal ISs were assessed. Examples are presented in Fig. 4A-C, where hippocampal LFP epochs were sampled from a single mouse at different experimental time points and spectral plots were derived from delta and theta segments including the epochs illustrated. Relative to baseline delta activity, there were minor-moderate changes in the peak frequencies of delta activity and corresponding powers following 50, 80, and ≥ 100 stimulations, while decreases in delta peak frequency and increases in corresponding power became evident following observation of early and late SRS (Fig. 4B). The latter spectral changes were in line with the rhythmic expression of ISs (Fig. 4A). Compared to the baseline theta rhythm, decreases in theta peak frequencies and/or powers were noticeable in both early and late SRS (Fig. 4C), which may be related to irregular expression of ISs (Fig. 4A).

Changes in delta and theta activities were assessed in the

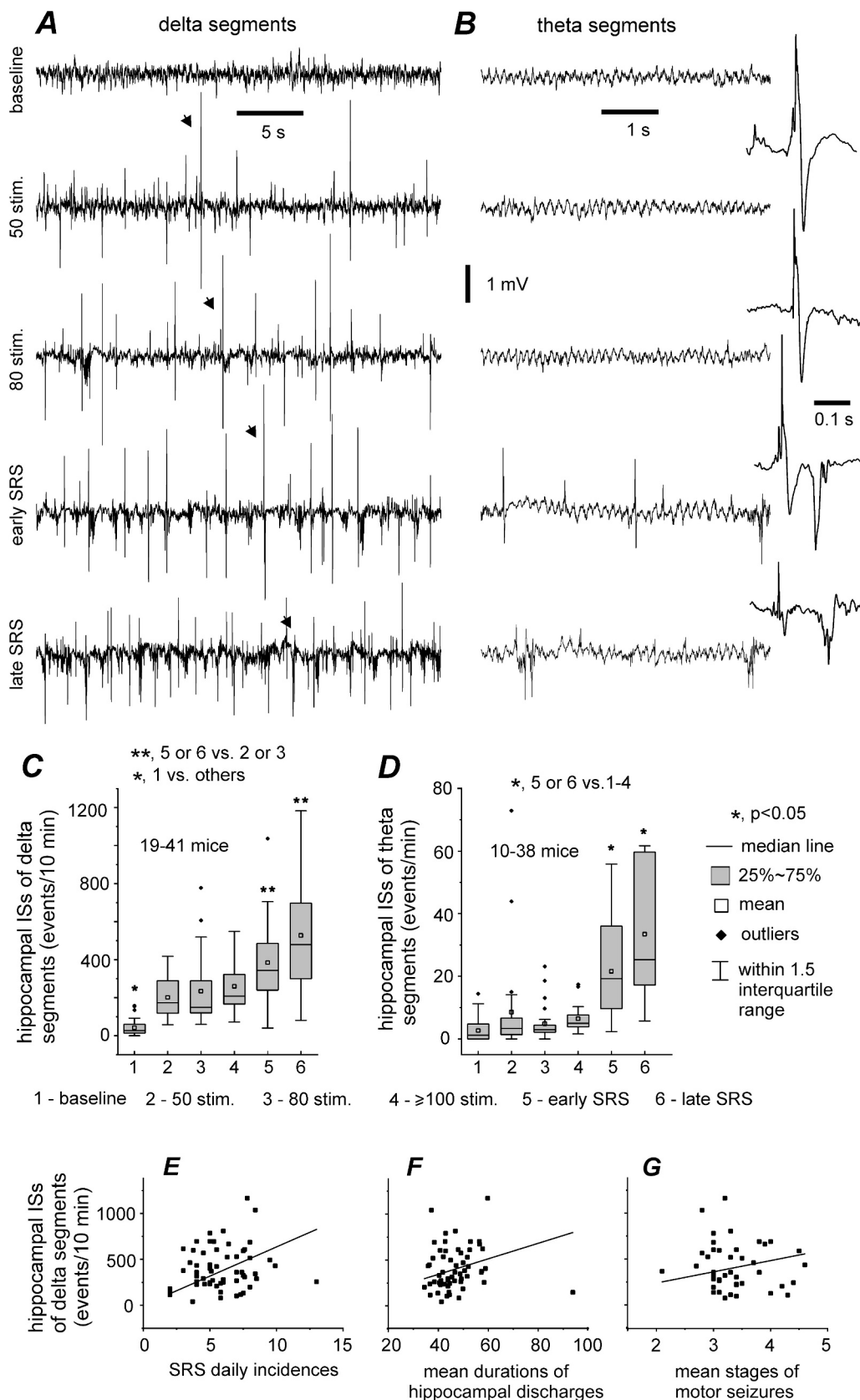


Fig. 3. Hippocampal ISs progressively increased following extended kindling. A-B, representative LFP epochs sampled from a mouse, showing spontaneous ISs at different experimental time points. Arrowed IS events expanded at far right. C–D, IS rates presented in box plots. Data collected before kindling (baseline), following 50, 80, and ≥ 100 stimulations, and after observation of early and late SRS. * or **, $p < 0.05$, nonparametric Kruskal-Wallis test. E–G, hippocampal IS rates of delta segments plotted against SRS daily incidences, mean durations of hippocampal discharges or mean stages of motor seizures. Data points measured from individual mice ($n = 48$ or 43). Lines through data points computed via linear regression function.

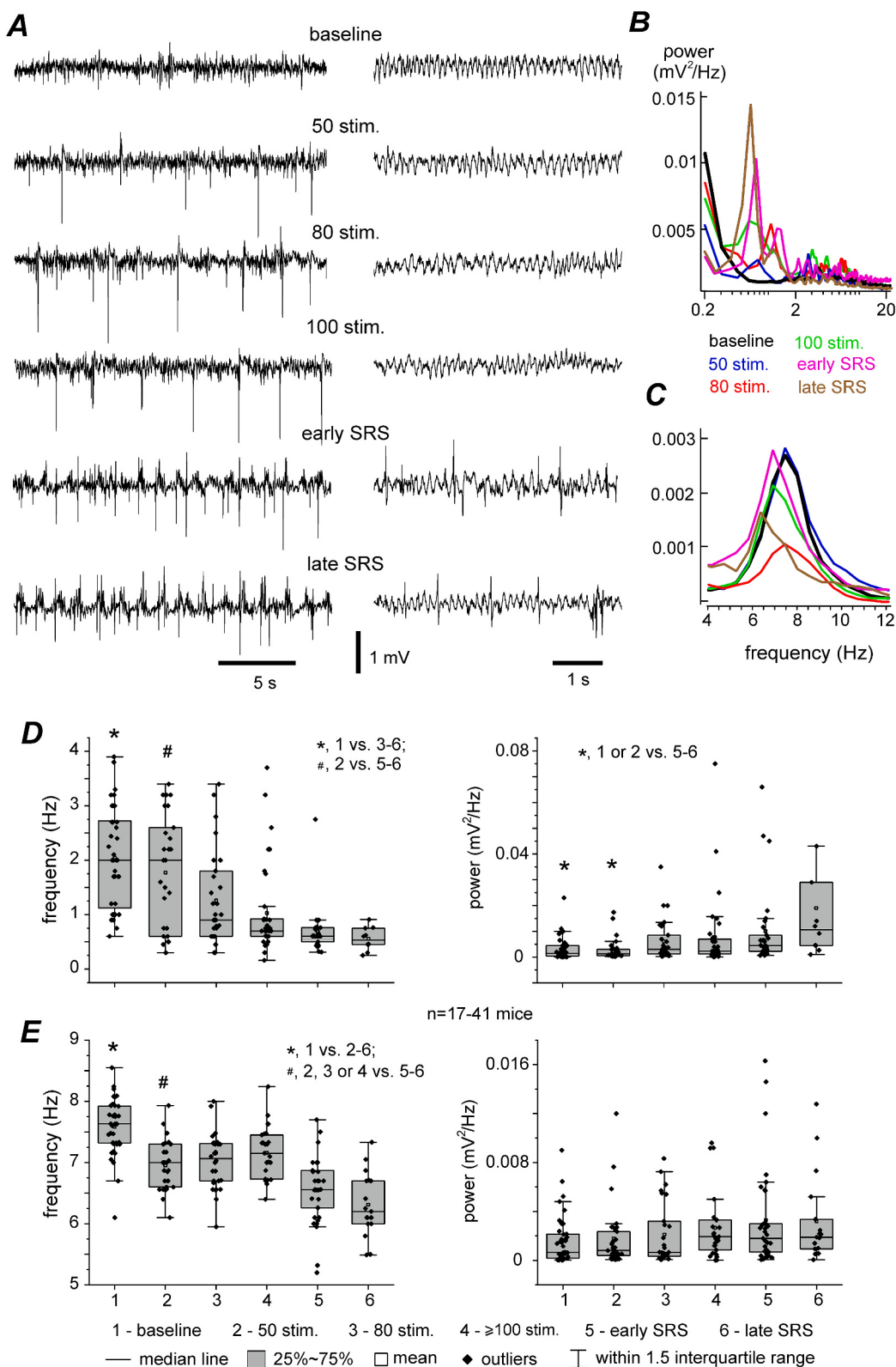


Fig. 4. Changes in hippocampal delta and theta activities. A, representative LFP epochs sampled from a mouse before kindling (baseline) and at different time points following kindling. B, spectral plots generated from delta segments including epochs illustrated in A. C, averaged spectral plots from 3 to 6 theta segments were presented for indicated experimental time points. In B and C, pre-kindling or baseline plots are denoted by black lines; plots corresponding to 50, 80 and > 100 stimulations (stim.) are indicated by blue, red and green lines respectively; plots matching early and late SRS are designated by purple and brown lines. D-E, frequencies and powers of hippocampal delta and theta activities assessed at different experimental time points. Data presented in box plot. * or #, p < 0.05, non-parametric Kruskal-Wallis test. (For interpretation of the references to colour in this figure legend, the reader is referred to the web version of this article.)

hippocampal-hippocampal, hippocampal-cortical, hippocampal-piriform, and hippocampal-entorhinal groups. The peak frequencies of delta activity were 2.04 ± 0.15 Hz before kindling (baseline), 1.77 ± 0.20 Hz, 1.26 ± 0.15 Hz, and 1.02 ± 0.14 Hz following respectively 50, 80, and ≥ 100 stimulations, 0.70 ± 0.07 Hz after early SRS, and 0.76 ± 0.17 Hz after late SRS. Delta frequencies did not vary from baseline after 50 stimulations but decreased significantly following both longer kindling (80 and ≥ 100 stimulations) and SRS occurrence (nonparametric Kruskal-Wallis test, $n = 27-40$ per group; Chi-square 51.3 or 18.4, df = 4, prob. > Chi-square < 0.0001; Dunn's test, $p < 0.05$; Fig. 4D). The powers corresponding to delta peak frequencies in the early and late SRS stages (0.0122 ± 0.0027 and 0.0159 ± 0.0073 Hz/mV₂, respectively) were significantly higher than those observed both at baseline and following 50 stimulations (0.003 ± 0.0008 and 0.0082 ± 0.0057 Hz/mV₂, respectively) (nonparametric Kruskal-Wallis test, Chi-square 18.4, df = 4, prob. > Chi-square = 0.00104; Dunn's test, $p < 0.05$; Fig. 4D).

The peak frequencies of theta rhythm were 7.58 ± 0.07 Hz at baseline, 6.95 ± 0.085 Hz, 7.02 ± 0.08 Hz, and 7.16 ± 0.09 Hz following 50, 80, and ≥ 100 stimulations, and 6.55 ± 0.09 Hz and 6.31 ± 0.13 Hz after observation of early and late SRS, respectively. All measures obtained following kindling were significantly decreased from the baseline measure, and a further significant reduction was noted after SRS occurrence (nonparametric Kruskal-Wallis test, $n = 10-37$ per group; Chi-square 61.3, df = 4, prob. > Chi-square < 0.0001; Dunn's test, $p < 0.05$; Fig. 4E). However, there was no significant difference among theta powers assessed at different experimental time points (Fig. 4F). Collectively, the above observations suggest that occurrences of hippocampal ISs are associated with changes in hippocampal delta and theta activities.

7. Analysis of IS-associated fast ripples (FRs)

To assess IS-associated FRs, hippocampal ISs detected from delta segments were treated with a band pass filter (250–500 Hz) and FR signals within ± 100 ms of corresponding ISs were analyzed. Fig. 5A-E presents examples of original and filtered ISs signals collected from a mouse following extended kindling, depicting noticeably weak FR signals after observation of SRS. To estimate the rates of IS-associated FRs in individual mice, the incidences of recognized FR events were normalized as percentiles of the total hippocampal ISs detected at different experimental time points, and data from mice in the hippocampal-hippocampal, hippocampal-cortical, hippocampal-piriform, and hippocampal-entorhinal groups were pooled together.

Overall, FR rates were quite variable following 50, 80, and ≥ 100 stimulations and upon development of early and late SRS. Although there were no significant differences among these FR rates, they were all significantly greater than the baseline measure (nonparametric Kruskal-Wallis test, $n = 17-41$ per group; Chi-square 26.2, df = 5, prob. > Chi-square < 0.0001; Dunn's test, $p > 0.05$ or $p < 0.05$; Fig. 5F). Therefore, these observations do not support in our model an association between SRS development and increased IS-associated FR rates.

8. ISs analysis in unstimulated forebrain structures

In our experiments, LFP recordings were made from the stimulated hippocampus as well as from unstimulated forebrain structures in individual mice. The latter areas included the contralateral hippocampus, and contralateral or ipsilateral parietal cortex, piriform cortex, entorhinal cortex, and dorsomedial thalamus. These unstimulated regions were selected to compare LFP signals between seizure-prone limbic (hippocampal, piriform, and entorhinal) and non-limbic (parietal cortical and thalamic) structures, according to previous kindling studies in monkeys and cats (Wada et al., 1974; Gotman, 1984; Gigli and Gotman, 1991; Hiyoshi et al., 1993). Corresponding regional ISs were assessed in delta segments and occurred predominantly during inactive

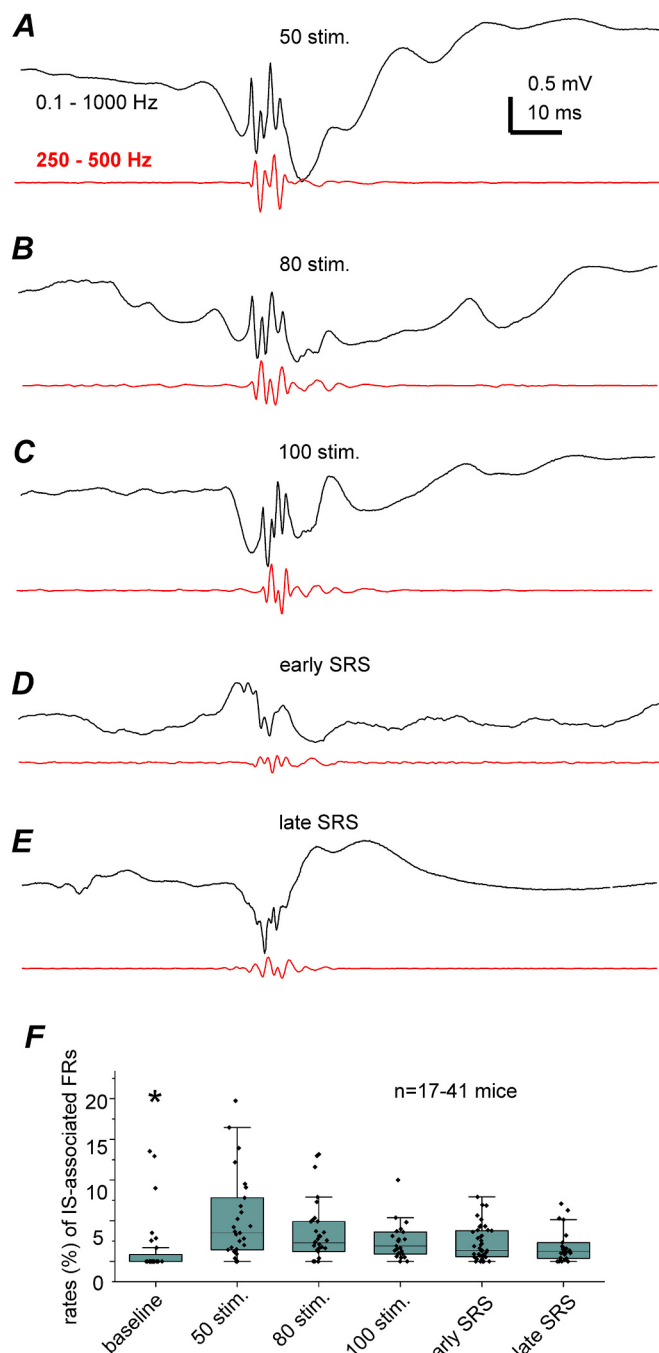


Fig. 5. Analysis of fast ripples (FRs) following kindling. A-E, representative epochs collected from a mouse before kindling (baseline) and at the indicated time points following kindling. Black traces illustrate signals recorded in the frequency band of 0.1–1000 Hz. Red traces represent the corresponding signals after treatment with a band passing filter (250–500 Hz). F, FRs associated with hippocampal ISs were normalized as percentiles of total hippocampal ISs detected from individual mice at the indicated experimental time points. Data presented in box plot. *, $p < 0.05$, nonparametric Kruskal-Wallis test, baseline vs. other measures. (For interpretation of the references to colour in this figure legend, the reader is referred to the web version of this article.)

behaviors. To assess temporal relations of regional ISs while minimizing complications derived from their multi-peak waveforms, the spike detection threshold was increased from 4 SD to 6 SD of the mean value of background signals. Corresponding regional ISs were considered coherent if their peaks occurred within a time window of ± 200 ms, with ISs of the stimulated hippocampus leading, coinciding with, or lagging

their counterparts based on their peak timings. Fig. 6 presents examples of LFP epochs showing coherent and non-coherent IS events between bilateral hippocampal, hippocampal-cortical, hippocampal-piriform, hippocampal-entorhinal, and hippocampal-thalamic ISs (Fig. 6A-E, left). Some coherent ISs were superimposed and expanded to illustrate leading or lagging hippocampal ISs relative to ISs arising in non-stimulated brain regions (Fig. 6A-E, right).

The expression of regional ISs was next assessed in the five groups of mice (Fig. 7). Data collected following 50, 80, and ≥ 100 stimulations (referred to as “kindling”) and after observation of early and late SRS (referred to as “SRS”) were separately pooled together because sample sizes were relatively small for individual experimental time points. Numbers of corresponding regional ISs (events/10 min) obtained from individual mice were linked with solid lines to illustrate the overall trend in each group (Fig. 7A-B). There was no significant difference between IS numbers recorded in stimulated and unstimulated regions in the hippocampal-hippocampal and hippocampal-piriform groups (paired *t*-test or Mann-Whitney *U* test; Fig. 7A-B). In contrast, the number of hippocampal ISs was significantly higher compared to that of cortical or thalamic ISs (Mann-Whitney *U* test, $n = 22$ or 29 , $u = 429$ or 814 , $z = 4.379$ or 6.124 , $p < 0.0001$, Fig. 7A-B). In addition, the number of unstimulated cortical and thalamic ISs was significantly smaller than that of unstimulated hippocampal or piriform ISs (nonparametric Kruskal-Wallis test, $n = 19$ - 28 ; Chi-square 59.65 , $df = 4$, prob. $>$ Chi-square < 0.0001 ; Dunn's test, $p < 0.05$; Fig. 7B). Measures from the hippocampal-entorhinal group were not included in the above comparison due to small sample size, although IS numbers in the corresponding stimulated and unstimulated regions also seemed comparable in this group.

To assess the rate of coherent regional ISs, their proportions were normalized as percentiles of the total ISs detected from the stimulated hippocampus or the unstimulated structure (whichever was lower), and normalized data were pooled together for mice in each group. Overall, the rates of coherent regional ISs were variable in individual groups. There were no significant group differences following kindling, but significantly greater rates for the hippocampal-piriform group ($78.7\% \pm 4.5\%$) relative to the hippocampal-hippocampal, hippocampal-cortical, and hippocampal-thalamic groups ($35.1\% \pm 5.0\%$, $33.8 \pm 6.0\%$, and $32.7\% \pm 10.0\%$, respectively) were noted after observation of SRS (nonparametric Kruskal-Wallis test, $n = 11$ - 33 per group; Chi-square 50.39 , $df = 7$, prob. $>$ Chi-square < 0.0001 ; Dunn's test, $p < 0.05$; Fig. 7C). The rates of coherent ISs in the hippocampal-entorhinal group were within the range of measures observed in the hippocampal-piriform group.

The proportions of leading hippocampal ISs relative to corresponding unstimulated regional ISs were normalized as percentiles of total coherent regional ISs (Fig. 7D). Following kindling and after observation of SRS, the rates of leading hippocampal ISs were respectively $69.9\% \pm 5.1\%$ and $71.8 \pm 6.3\%$ for the hippocampal-cortical group, $50.6\% \pm 10.4\%$ and $35.3\% \pm 6.0\%$ for the hippocampal-piriform group, and $48.7\% \pm 4.9\%$ and $51.1\% \pm 4.2\%$ for the bilateral hippocampal group. The measures from the hippocampal-cortical group were significantly different from those of the hippocampal-piriform, but not the bilateral hippocampal group (nonparametric Kruskal-Wallis test; $n = 11$ - 32 per group; Chi-square 18.36 , $df = 5$, prob. $>$ Chi-square $= 0.0025$; Dunn's test, $p < 0$ or > 0.05 ; Fig. 7D). The rates of leading hippocampal ISs in the hippocampal-entorhinal group were $\geq 78\%$, except one case. Collectively, these observations suggest that among the unstimulated limbic and non-limbic structures examined, the former structures have greater probability of generating ISs.

9. Discussion

9.1. SRS development accompanied with increased hippocampal ISs

A consistent observation in our present analysis was an overall

increase in the rate of kindling related hippocampal ISs upon SRS development. The ISs detected from both delta and theta segments after observation of early and late SRS were significantly more numerous than those following extended kindling but prior to SRS occurrence, whereas gradually increased IS rates with extended kindling was evident in measures from delta, but not theta segments. Collectively, these observations indicate a close association of increased IS activity with SRS development in our kindling model, which is in line with previous finding in rats with kainate-induced SRS (White et al., 2010). Previous studies in amygdala kindled cats have shown prolonged increases or decreases in IS rates following an event of evoked seizures or SRS (Gotman, 1984; Gigli and Gotman, 1991). This phenomenon was not evident in hippocampal kindled mice. We found that while hippocampal IS signals were evidently suppressed for a few min following each SRS event, ISs that occurred subsequently prior to next SRS were relatively stable in their incidences when monitored over a time window of up to several hours. The discrepancy between the previous findings (Gotman, 1984; Gigli and Gotman, 1991) and our present observations may be due to multiple factors including differences in animal species, kindling sites and incidences of kindling-induced SRS.

Epileptic network activity involving dynamic interplays of synaptic activities (mainly glutamatergic and GABAergic) and non-synaptic activities, as well as other factors, are thought to underlie the genesis and progression of ISs (de Curtis and Avanzini, 2001; Avoli et al., 2022). Similar epileptic network activity may operate to generate hippocampal ISs in kindled mice. While details of such network activity underlying kindling-induced ISs at different time points of hippocampal kindling remain to be investigated, our present observations provide evidence regarding the influence of behavioral state-dependent background network activities on IS activity. The rodent hippocampus exhibits large- or small-amplitude irregular activity of ≤ 4 Hz during inactive behaviors such slow wave sleep or stable immobility, and theta rhythm of 5-12 Hz during active behaviors including exploration and movement as well as alert immobility (Vanderwolf, 1969; Leung et al., 1982; Jarosiewicz et al., 2002; Buzsáki, 2002, 2015; Mysin and Shubina, 2023). Intermingled with the irregular activity are intermittent sharp waves that are often associated with physiological ripples (80-200 Hz; Buzsáki, 2015). The sharp waves are thought to be primarily originated from the hippocampal CA3 circuit, as the influences of extra-hippocampal inputs on the CA3 activity are reduced during the inactive behaviors. In contrary, extra-hippocampal inputs play critical roles in the generation of hippocampal theta rhythm (Buzsáki, 2002, 2015). The CA3 circuit also plays important roles in the generation of hippocampal theta rhythm and epileptiform activity (Le Duigou et al., 2014). We thus monitored hippocampal ISs from the CA3 area of kindled mice. Based on the above information, it is conceivable that inactive behaviors with dominant background delta activity are favorable for genesis of hippocampal ISs relative to active behaviors with dominant theta rhythm. This would mainly account for the progressively increased IS rates in delta but not theta segments.

9.2. IS occurrences associated with alterations of hippocampal delta and theta activity

Accompanying the progressive increase in IS rates was a gradual decrease in the frequencies of delta activity. In particular, spectral analyses showed that mean peak frequencies of delta activity decreased to about 0.5 Hz, while their corresponding powers increased, after observations of SRS. These spectral changes may be related to the occurrence of frequent ISs as spectral plots were generated from delta segments that encompassed strong and periodic IS signals. It is possible that the inhibitory activity following ISs (de Curtis and Avanzini, 2001) may help entrain hippocampal network activity, which in return may enforce the rhythmic expression of ISs hence largely accounting for the decrease in delta frequency observed.

Relative to the baseline measure, the peak frequencies of

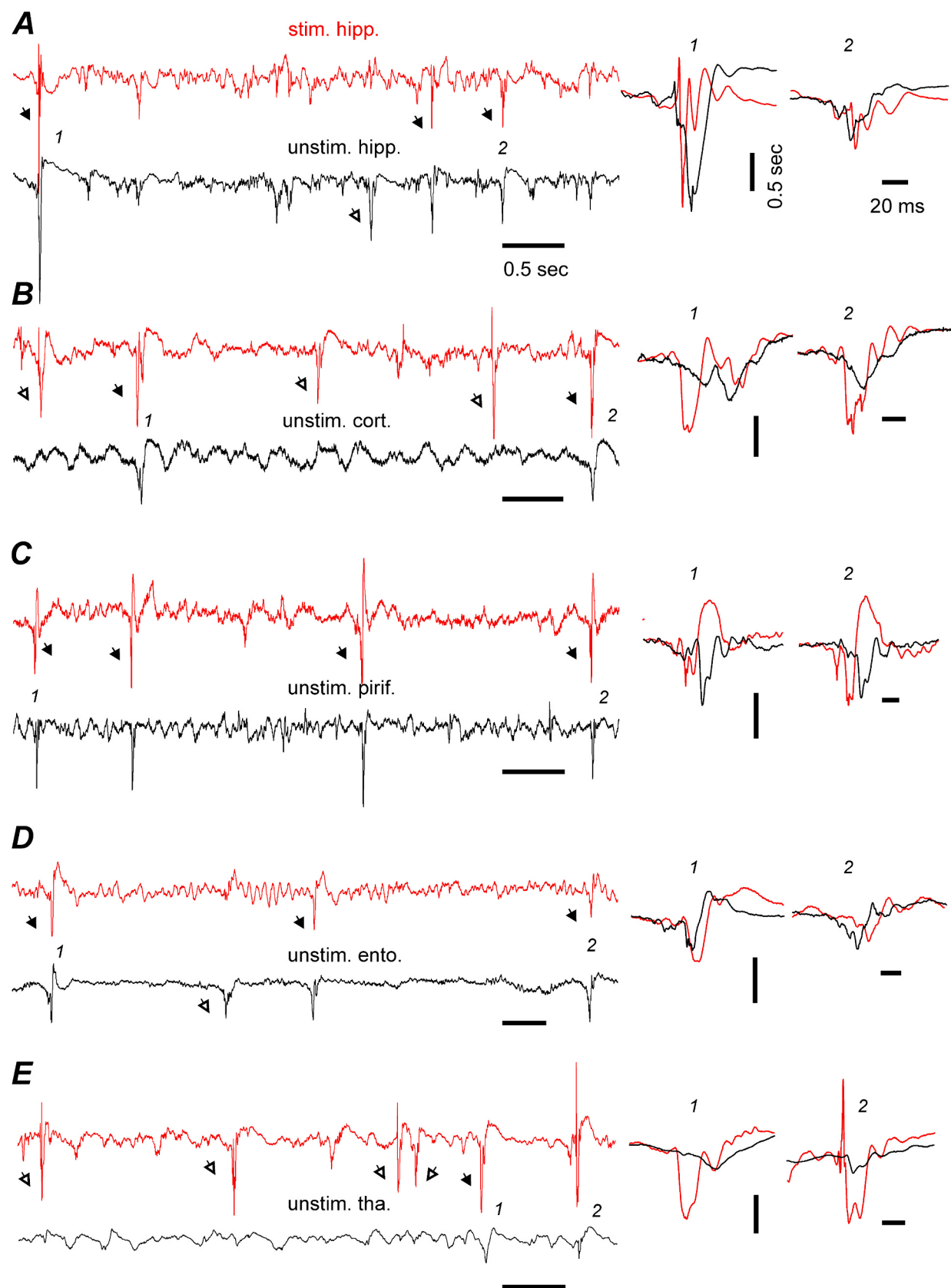
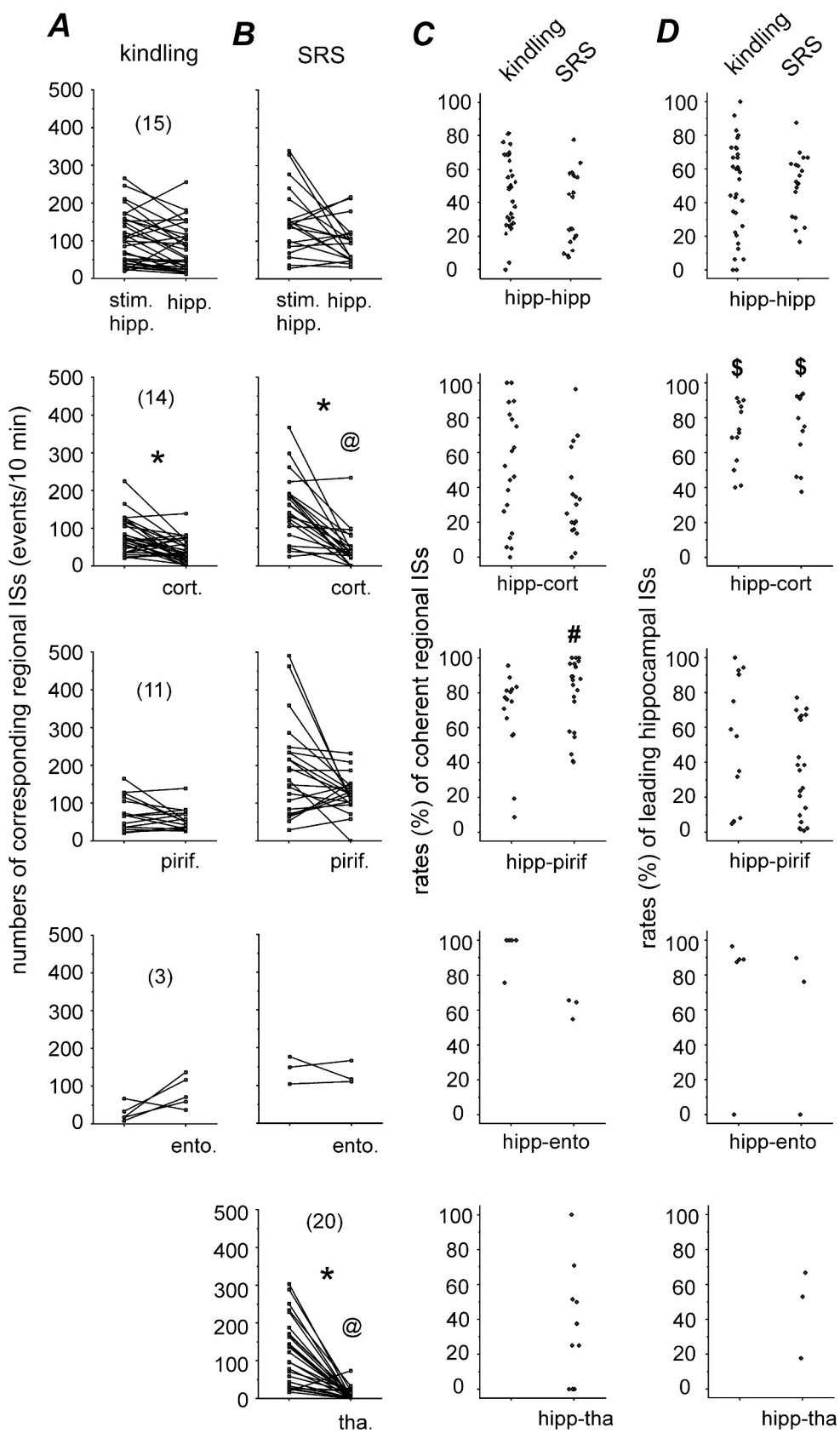


Fig. 6. Examples of regional IS expression. LFP epochs were collected from five mice (A-E) following 80 kindling stimulations (A-D) or after observation of early SRS (E). Top (red), LFPs from stimulated hippocampus (stim. Hipp.). Bottom (black), LFPs simultaneously recorded from unstimulated (unstim.) hippocampus, parietal cortex (cort.), piriform cortex (pirif.), entorhinal cortex (ento.), and dorsomedial thalamus (tha.). Coherent and non-coherent regional ISs are denoted by filled and open arrows, respectively. Numbered events were superimposed and expanded to show peak timing (right). (For interpretation of the references to colour in this figure legend, the reader is referred to the web version of this article.)



(caption on next page)

Fig. 7. Analysis of regional IS rates. ISs of delta segments measured from the stimulated hippocampus and unstimulated hippocampus (hipp.), parietal cortex (cort.), piriform cortex (pirif.), entorhinal cortex (ento.), and dorsomedial thalamus (tha.). Numbers of mice examined in each group indicated in parentheses. Group comparisons were made by nonparametric Kruskal-Wallis test, excluding data from the hippocampal-entorhinal group due to small sample size. A-B, numbers of detected regional ISs. Corresponding measures from individual mice linked by solid lines. *, p < 0.05, stimulated hippocampal ISs vs. unstimulated regional ISs. @, p < 0.05, unstimulated thalamic ISs vs. unstimulated hippocampus/piriform ISs or unstimulated cortical ISs vs. piriform ISs. C, rates of coherent regional ISs. Data presented as percentage of total ISs detected from the stimulated hippocampus or a simultaneously assessed unstimulated structure, whichever was lower. #, p < 0.05, rates of coherent hippocampal and piriform ISs vs. others. D, rates of leading hippocampal ISs relative to unstimulated regional ISs. Data presented as percentage of total coherent regional ISs for each group. \$, p < 0.05, rates of leading hippocampal ISs in the hippocampal-cortical group vs. the hippocampal-piriform group.

hippocampal theta rhythm were significantly reduced following extended kindling and decreased further after observation of early and late SRS. These observations are in keeping with findings from other epilepsy models (Chauvière et al., 2009; Milikovsky et al., 2017; Kilias et al., 2018), further suggesting that disruptions in theta rhythm are an early sign of epileptogenesis in the kindling model. After SRS onset, the decrease in theta frequencies accompanying the occurrence of hippocampal ISs may also suggest a negative impact of ISs on theta rhythm (Ge et al., 2013). However, as theta segments were collected while mice were largely immobile, these segments might mainly encompass the atropine-sensitive type 2 theta rhythm (Bland et al., 2007; Mocellin and Mikulovic, 2021). While such data selection helped minimize the complications of movement-related artifacts on IS detection, further work is needed to verify the changes in hippocampal theta rhythm in our model by testing the effects of atropine and correlating theta rhythm with inactive or active behaviors.

9.3. IS expressions differed among unstimulated limbic and non-limbic structures

In our experiments, simultaneous LFP recordings from the stimulated hippocampus and from one of five unstimulated forebrain structures were made in individual mice. Following extended kindling and after SRS onset, different spontaneous IS rates were detected in the unstimulated limbic (hippocampus, piriform cortex, and entorhinal cortex) and non-limbic (parietal cortex and dorsomedial thalamus) structures. These observations, although obtained from different groups of mice, are in general agreement with previous kindling studies that demonstrated occurrence of ISs in forebrain structures of individual monkeys and cats (Wada et al., 1974; Gotman, 1984; Gigli and Gotman, 1991; Hiyoshi et al., 1993). Following extended kindling and after observation of SRS, the numbers of regional ISs were comparable between the stimulated hippocampus and the unstimulated contralateral hippocampus and piriform and entorhinal cortices. In contrast, the unstimulated cortex and thalamus expressed significantly fewer ISs compared to the stimulated hippocampus, the unstimulated hippocampus, and the unstimulated piriform cortex. Still, variabilities in the estimated rates of coherent regional ISs and leading hippocampal ISs were largely comparable in the five of groups of mice. These data suggest that the unstimulated limbic structures have higher probability to generate ISs relative to the unstimulated non-limbic structures, although both types of structures can generate ISs either dependently or independently of hippocampal stimulation. Our study thus provides original information about regional IS expression before and after SRS occurrence in a kindling model.

Distinct regional expressions of IS and ictal discharges were noted in our model, as the ictal discharges always concurred in the stimulated hippocampus and co-recorded unstimulated structures, featuring similar low voltage fast signals at onset (Liu et al., 2021). It seems therefore that epileptic network activity involving multiple forebrain structures is responsible for initiating ictal discharges, whereas local epileptic network activities can generate ISs relatively independently. In this regard, our previous research showed that treatments with clinically used antiepileptic drugs abolished ictal discharges but not ISs in our model (Song et al., 2018). Collectively, these data support the view that different but interrelated epileptic network activities may underlie the

genesis of ictal discharges and ISs in the kindling model (Gotman, 1984; Gigli and Gotman, 1991; Hiyoshi et al., 1993) and other epilepsy models (de Curtis and Avanzini, 2001; Avoli et al., 2022).

9.4. Variable expressions of hippocampal complex ISs and IS-associated FRs

In our experiments, individual mice consistently exhibited hippocampal ISs with simple or complex waveforms when examined at different time points following kindling. Our present observations agree with previous studies in animals that underwent classical kindling (Kairiss et al., 1984; Racine et al., 1988; Sobieszek, 1989; Leung, 1990, 1994; Kogure, 1997) or extended kindling (Wada and Osawa, 1976; Pinel and Rovner, 1978b; Gotman, 1984; Gigli and Gotman, 1991; Brandt et al., 2004; Song et al., 2018). The genesis of complex ISs appears to be a common feature of the kindling models and a result of chronic kindling stimulations, as consistent expression of ISs with complex waveforms has not, to our knowledge, been reported for other epilepsy models. However, the expressions of complex ISs were highly variable in individual mice, and their rates did not differ before and after SRS occurrence. Likewise, rates of FRs associated with hippocampal ISs were also highly variable in individual mice, showing also no significant differences following extended kindling and after SRS onset. The lack of increased FR rates with SRS development in our model is unexpected, as SRS development was accompanied with marked increases in hippocampal IS rates. The reasons behind the lack of association between SRS development and increased rates of complex ISs or FRs are unclear, but relevant experimental confounds are worthy of discussion.

Previous studies have recorded spontaneous ISs from the hippocampal CA1 region of classically kindled animals (Kairiss et al., 1984; Morimoto et al., 1987; Leung, 1994; Kogure, 1997). The waveform and polarity of CA1 ISs were found to be dependent on the locations of the recording electrodes in CA1 sub-regions. ISs with poly-spike waveforms appeared to be optimally captured by recordings from or near the CA1 cell body layer. In addition, hippocampal physiological ripples recorded from the CA1 regions were more prominent in the cell body layer relative to the apical dendritic layer (Buzsáki, 2015). In our experiments, we aimed to record LFPs from the CA3 region of the middle hippocampus, but the locations of CA3 electrodes were not determined histologically in all the mice examined. Moreover, in the mice in which histology was performed, the exact locations of putative electrode tips in CA3 sub-regions were often difficult to determine (Liu et al., 2021). Hence, uncertainty regarding electrode placement might have contributed to the variability and/or potential underestimation of the rates of multi-peak complex ISs and/or FRs. In addition, we made repeated LFP recordings from individual mice over the course of a few months. LFP signals were noticeably attenuated when monitored in the later than in the early experimental time points. Such attenuation was likely due to increased electrode impedance because of electrode tip contaminations over a prolonged implantation period. The increase in electrode impedance may lead to weak LFPs, and as high frequency signals are generally attenuated more than low frequency signals, FR signals in particular may have been more difficult to detect. This may partly explain the relatively high FR rates observed in some mice following 50 stimulations but not at later experimental time points.

Previous studies in the rat model of classic kindling have shown that

prolonged implantation of intracranial electrode enhanced kindling rates, reduced evoked after-discharge thresholds and altered GABA turnover signals (Blackwood et al., 1982; Löscher et al., 1995, 1999). Impacts of prolonged electrodes implantation have been recognized in other rodent models of epilepsy (Bankstahl et al., 2014; Tse et al., 2021). In our experiments, each mouse received implantation of two pairs of bipolar electrodes and underwent kindling stimulation and LFP recordings over a few months. Such prolonged electrode implantation might have significant effects on SRS and ISs observed from individual mice. In addition, local lesions or irritations resulting from electrode implantation might have contributed to occurrence of spontaneous spikes observed in the control mice and in mice before hippocampal kindling. Future experiments are needed to assess acute and chronic effects of electrode implantation and to further characterize our model.

9.5. Clinical relevance and future direction

Our present data are clinically relevant in several aspects. Hippocampal ISs with heterogeneous morphologies have been observed in patients with temporal lobe epilepsy that underwent pre-surgical assessments via intracranial LFP recordings. These ISs displayed negative or positive polarity, monophasic or biphasic waveform with or without a post-spike wave component (Issa et al., 2018; Epitashvili et al., 2021; Bruzzone et al., 2022). The simple and complex hippocampal ISs we observed from kindled mice are in keeping with these clinical findings. In addition, EEG abnormalities including ISs, sharp waves and/or spiky periodic discharges are thought to be a risk factor for seizure recurrence after stroke or traumatic brain injury (Bentes et al., 2018; Chen et al., 2021; Abe et al., 2022). Our observations of increased hippocampal ISs during SRS development in kindled mice are in line with this view. Moreover, elevated theta rhythms are thought to represent a seizure-resistant network activity state, and promoting theta rhythm by electrical stimulation of the medial septum has been hypothesized as a novel treatment approach for refractory epilepsy (Izadi et al., 2018, 2019, 2021; Cole et al., 2022). Our observations that hippocampal theta activity was decreased and associated with infrequent ISs during SRS development are in conformity with this hypothesis. It has been increasingly recognized that interictal epileptiform discharges interrupt memory processes, hence being significant contributors to cognitive comorbidity (Ung et al., 2017; Henin et al., 2021; Quon et al., 2021; Meisenhelter et al., 2021; Camarillo-Rodriguez et al., 2022). Increased IS activity and decreased hippocampal rhythmicity may be significant contributing factors to spatial memory impairment observed in kindled mice (Liu et al., 2019).

In summary, despite of the abovementioned and other limitations, our present study provides original evidence indicating that SRS development is accompanied with increases in the rates of hippocampal ISs and decreases in the frequencies of hippocampal delta and theta activities in the mouse model of kindling-induced epilepsy. Our present data provide a framework for further examination of the mechanisms that may underlie IS genesis in temporal lobe epilepsy.

Supplementary data to this article can be found online at <https://doi.org/10.1016/j.expneurol.2024.114860>.

Funding

This work has been funded by a grant from the Epilepsy Research Program of Ontario Brain Institute and supported by Program of Provincial Science and Technology Development of Jilin, China (No.20210402008GH).

Institutional review board statement

All experimentations were reviewed and approved by the Animal Care Committee of University Health Network (Animal User Protocol 986.40) according to the Guidelines of the Canadian Council on Animal

Care.

Informed consent statement

Not applicable.

CRedit authorship contribution statement

Hongmei Song: Project administration, Methodology, Investigation. **Bryan Mah:** Writing – review & editing, Data curation. **Yuqing Sun:** Data curation. **Nancy Aloysius:** Data curation. **Yang Bai:** Funding acquisition, Conceptualization. **Liang Zhang:** Writing – original draft, Validation, Supervision, Investigation, Funding acquisition, Conceptualization.

Declaration of competing interest

The authors declare that they have no known competing financial interests or personal relationships that could have appeared to influence the work reported in this paper.

Data availability

The data presented in this study are available within the article.

References

- Abe, S., Tanaka, T., Fukuma, K., Matsubara, S., Motoyama, R., Mizobuchi, M., Yoshimura, H., Matsuki, T., Manabe, Y., Suzuki, J., Ishiyama, H., Tojima, M., Kobayashi, K., Shimotake, A., Nishimura, K., Koga, M., Toyoda, K., Murayama, S., Matsumoto, R., Takahashi, R., Ikeda, A., Ihara, M., 2022. PROPOSE study investigators. Interictal epileptiform discharges as a predictive biomarker for recurrence of poststroke epilepsy. *Brain Commun.* 4 (6), fcac312.
- Avoli, M., de Curtis, M., Lévesque, M., Librizzi, L., Uva, L., Wang, S., 2022. GABA signaling, focal epileptiform synchronization and epileptogenesis. *Front Neural Circuits*, 16, 984802.
- Bajorat, R., Goerss, D., Brenndörfer, L., Schwabe, L., Köhling, R., Kirschstein, T., 2016. Interplay between interictal spikes and behavioral seizures in young, but not aged pilocarpine-treated epileptic rats. *Epilepsy Behav.* 57 (Pt A), 90–94.
- Bankstahl, J.P., Brandt, C., Löscher, W., 2014. Prolonged depth electrode implantation in the limbic system increases the severity of status epilepticus in rats. *Epilepsy Res.* 108 (4), 802–805.
- Bentes, C., Martins, H., Peralta, A.R., Morgado, C., Casimiro, C., Franco, A.C., Fonseca, A. C., Geraldes, R., Canhão, P., Melo, Pinho E., Paiva, T., Ferro, J.M., 2018. Early EEG predicts poststroke epilepsy. *Epilepsia Open* 3 (2), 203–212.
- Bin, N.R., Song, H., Wu, C., Lau, M., Sugita, S., Eubanks, J.H., Zhang, L., 2017. Continuous monitoring via tethered electroencephalography of spontaneous recurrent seizures in mice. *Front. Behav. Neurosci.* 2017, 11:172.
- Blackwood, D.H., Martin, M.J., McQueen, J.K., 1982. Enhanced rate of kindling after prolonged electrode implantation into the amygdala of rats. *J. Neurosci. Methods* 5 (4), 343–348.
- Bland, B.H., Derie-Gillespie, D., Mestek, P., Jackson, J., Crooks, R., Cormican, A., 2007. To move or not: previous experience in a runway avoidance task determines the appearance of hippocampal type 2 sensory processing theta. *Behav. Brain Res.* 179, 299–304.
- Bragin, A., Wilson, C.L., Almajano, J., Mody, I., Engel Jr., J., 2004. High-frequency oscillations after status epilepticus: epileptogenesis and seizure genesis. *Epilepsia* 45 (9), 1017–1023.
- Brandt, C., Ebert, U., Löscher, W., 2004. Epilepsy induced by extended amygdala-kindling in rats: lack of clear association between development of spontaneous seizures and neuronal damage. *Epilepsy Res.* 62 (2–3), 135–156.
- Bruzzone, M.J., Issa, N.P., Wu, S., Rose, S., Esengul, Y.T., Towle, V.L., Nordli, D., Warnke, P.C., Tao, J.X., 2022. Hippocampal spikes have heterogeneous scalp EEG correlates important for defining IEDs. *Epilepsy Res.* 182, 106914.
- Buzsáki, G., 2002. Theta oscillations in the hippocampus. *Neuron* 33 (3), 325–340.
- Buzsáki, G., 2015. Hippocampal sharp wave-ripple: a cognitive biomarker for episodic memory and planning. *Hippocampus* 25 (10), 1073–1188.
- Camarillo-Rodriguez, L., Leenen, I., Waldman, Z., Serruya, M., Wanda, P.A., Herweg, N. A., Kahana, M.J., Rubinstein, D., Orosz, I., Lega, B., Podkorytova, I., Gross, R.E., Worrell, G., Davis, K.A., Jobst, B.C., Sheth, S.A., Weiss, S.A., Sperling, M.R., 2022. Temporal lobe interictal spikes disrupt encoding and retrieval of verbal memory: a subregion analysis. *Epilepsia* 63 (9), 2325–2337.
- Chauvière, L., Rafrafi, N., Thénin-Blanc, C., Bartolomei, F., Escalpez, M., Bernard, C., 2009. Early deficit in spatial memory and theta rhythm in experimental temporal lobe epilepsy. *J. Neurosci.* 29 (17), 5402–5410.
- Chauvière, L., Doublet, T., Ghestem, A., Siyoucef, S.S., Wendling, F., Huys, R., Jirsa, V., Bartolomei, F., Bernard, C., 2012. Changes in interictal spike features precede the onset of temporal lobe epilepsy. *Ann. Neurol.* 71 (6), 805–814.

- Chen, D.F., Kumari, P., Haider, H.A., Ruiz, A.R., Lega, J., Dhakar, M.B., 2021. Association of epileptiform abnormality on electroencephalography with development of epilepsy after acute brain injury. *Neurocrit. Care.* 35 (2), 428–433.
- Cole, E.R., Grogan, D.P., Laxpati, N.G., Fernandez, A.M., Skelton, H.M., Isbaine, F., Gutekunst, C.A., Gross, R.E., 2022. Evidence supporting deep brain stimulation of the medial septum in the treatment of temporal lobe epilepsy. *Epilepsia* 63 (9), 2192–2213.
- de Curtis, M., Avanzini, G., 2001. Interictal spikes in focal epileptogenesis. *Prog. Neurobiol.* 63 (5), 541–567.
- Drexel, M., Rahimi, S., Sperk, G., 2022. Silencing of hippocampal somatostatin interneurons induces recurrent spontaneous limbic seizures in mice. *Neuroscience* 487, 155–165.
- El-Hayek, Y.H., Wu, C., Ye, H., Wang, J., Carlen, P.L., Zhang, L., 2013. Hippocampal excitability is increased in aged mice. *Exp. Neurol.* 247, 710–719.
- Engel Jr., J., Pitkänen, A., 2020. Biomarkers for epileptogenesis and its treatment. *Neuropharmacology* 167, 107735.
- Epitashvili, N., San Antonio-Arce, V., Brandt, A., Schulze-Bonhage, A., 2021. Intracranial correlates of small sharp spikes. *Clin. Neurophysiol.* 132 (9), 2146–2151.
- Ferlazzo, E., Sueri, C., Gasparini, S., Aguglia, U., 2016. Challenges in the pharmacological management of epilepsy and its causes in the elderly. *Pharmacol. Res.* 106, 21–26.
- Flurkey, K., Currer, J.M., Harrison, D.E., 2007. Mouse models in aging research. In: Fox, J.G., Davison, M.T., Quimby, F.W., et al. (Eds.), *The Mouse in Biomedical Research*, , 2nd edition3. Academic Press, pp. 637–672.
- Franklin, K.B., Paxinos, G., 1997. *The Mouse Brain in Stereotaxic Coordinates*. Academic Press, San Diego.
- Ge, M., Wang, D., Dong, G., Guo, B., Gao, R., Sun, W., Zhang, J., Liu, H., 2013. Transient impact of spike on theta rhythm in temporal lobe epilepsy. *Exp. Neurol.* 250, 136–142.
- Gigli, G.L., Gotman, J., 1991. Effects of seizures and carbamazepine on interictal spiking in amygdala kindled cats. *Epilepsy Res.* 8 (3), 204–212.
- Gorter, J.A., van Vliet, E.A., Lopes da Silva, F.H., 2016. Which insights have we gained from the kindling and post-status epilepticus models? *J. Neurosci. Methods* 260, 96–108.
- Gotman, J., 1984. Relationships between triggered seizures, spontaneous seizures, and interictal spiking in the kindling model of epilepsy. *Exp. Neurol.* 84 (2), 259–273.
- Henin, S., Shankar, A., Borges, H., Flinck, A., Doyle, W., Friedman, D., Devinsky, O., Buzsáki, G., Liu, A., 2021. Spatiotemporal dynamics between interictal epileptiform discharges and ripples during associative memory processing. *Brain* 144 (5), 1590–1602.
- Hiyoshi, T., Seino, M., Kakegawa, N., Higashi, T., Yagi, K., Wada, J.A., 1993. Evidence of secondary epileptogenesis in amygdaloid overkindled cats: electroclinical documentation of spontaneous seizures. *Epilepsia* 34 (3), 408–415, 8504775.
- Issa, N.P., Wu, S., Rose, S., Towle, V.L., Warnke, P.C., Tao, J.X., 2018. Small sharp spikes as EEG markers of mesiotemporal lobe epilepsy. *Clin. Neurophysiol.* 129 (9), 1796–1803.
- Izadi, A., Ondek, K., Schedlbauer, A., Keselman, I., Shahlaie, K., Gurkoff, G., 2018. Clinically indicated electrical stimulation strategies to treat patients with medically refractory epilepsy. *Epilepsia Open* 3 (Suppl. 2), 198–209.
- Izadi, A., Pevzner, A., Lee, D.J., Ekstrom, A.D., Shahlaie, K., Gurkoff, G.G., 2019. Medial septal stimulation increases seizure threshold and improves cognition in epileptic rats. *Brain Stimul.* 12 (3), 735–742.
- Izadi, A., Schedlbauer, A., Ondek, K., Disse, G., Ekstrom, A.D., Cowen, S.L., Shahlaie, K., Gurkoff, G.G., 2021. Early intervention via stimulation of the medial septal nucleus improves cognition and alters markers of epileptogenesis in pilocarpine-induced epilepsy. *Front. Neurol.* 12, 708957.
- Jarosiewicz, B., McNaughton, B.L., Skaggs, W.E., 2002. Hippocampal population activity during the small-amplitude irregular activity state in the rat. *J. Neurosci.* 22, 1373–1384.
- Kairiss, E.W., Racine, R.J., Smith, G.K., 1984. The development of the interictal spike during kindling in the rat. *Brain Res.* 322 (1), 101–110.
- Kilias, A., Häussler, U., Heining, K., Froriep, U.P., Haas, C.A., Egert, U., 2018. Theta frequency decreases throughout the hippocampal formation in a focal epilepsy model. *Hippocampus* 28 (6), 375–391.
- Kogure, S., 1997. Properties of interictal discharges induced by hippocampal kindling. *Epilepsia Res.* 27 (2), 139–148.
- Le Duigou, C., Simonnet, J., Telenčuk, M.T., Fricker, D., Miles, R., 2014. Recurrent synapses and circuits in the CA3 region of the hippocampus: an associative network. *Front. Cell. Neurosci.* 7, 262.
- Leung, L.W., 1990. Spontaneous hippocampal interictal spikes following local kindling: time-course of change and relation to behavioral seizures. *Brain Res.* 513 (2), 308–314. Apr 16.
- Leung, L.W., 1994. Evaluation of the hypothesis that hippocampal interictal spikes are caused by long-term potentiation. *Epilepsia* 35 (4), 785–794. Jul-Aug.
- Leung, L.W., Lopes da Silva, F.H., Wadman, W.J., 1982. Spectral characteristics of the hippocampal EEG in the freely moving rat. *Electroencephalogr. Clin. Neurophysiol.* 54, 203–219.
- Lévesque, M., Salami, P., Gotman, J., Avoli, M., 2012. Two seizure-onset types reveal specific patterns of high-frequency oscillations in a model of temporal lobe epilepsy. *J. Neurosci.* 32 (38), 13264–13272.
- Lévesque, M., Behr, C., Avoli, M., 2015. The anti-ictogenic effects of levetiracetam are mirrored by interictal spiking and high-frequency oscillation changes in a model of temporal lobe epilepsy. *Seizure* 25, 18–25.
- Lévesque, M., Biagini, G., de Curtis, M., Gnatakovsky, V., Pitsch, J., Wang, S., Avoli, M., 2021a. The pilocarpine model of mesial temporal lobe epilepsy: over one decade later, with more rodent species and new investigative approaches. *Neurosci. Biobehav. Rev.* 130, 274–291.
- Lévesque, M., Macey-Dare, A.D.B., Wang, S., Avoli, M., 2021b. Evolution of interictal spiking during the latent period in a mouse model of mesial temporal lobe epilepsy. *Curr Res Neurobiol.* 2, 100008.
- Lévesque, M., Wang, S., Macey-Dare, A.D.B., Salami, P., Avoli, M., 2023. Evolution of interictal activity in models of mesial temporal lobe epilepsy. *Neurobiol. Dis.* 180, 106065.
- Li, L., Patel, M., Almajano, J., Engel Jr., J., Bragin, A., 2018. Extrahippocampal high-frequency oscillations during epileptogenesis. *Epilepsia* 59 (4), e51–e55.
- Liu, H., Stover, K.R., Sivananthiran, N., Chow, J., Cheng, C., Liu, Y., Lim, S., Wu, C., Weaver, D.F., Eubanks, J.H., Song, H., Zhang, L., 2019. Impaired spatial learning and memory in middle-aged mice with kindling-induced spontaneous recurrent seizures. *Front. Pharmacol.* 10, 1077.
- Liu, H., Tufa, U., Zahra, A., Chow, J., Sivananthiran, N., Cheng, C., Liu, Y., Cheung, P., Lim, S., Jin, Y., Mao, M., Sun, Y., Wu, C., Wennberg, R., Bardakjian, B., Carlen, P.L., Eubanks, J.H., Song, H., Zhang, L., 2021. Electrographic features of spontaneous recurrent seizures in a mouse model of extended hippocampal kindling. *Cereb Cortex Comm* 2 (1), tgb004.
- Löscher, W., 2017. Animal models of seizures and epilepsy: past, present, and future role for the discovery of Antiseizure drugs. *Neurochem. Res.* 42 (7), 1873–1888.
- Löscher, W., Wahnschaffe, U., Hönnack, D., Rundfeldt, C., 1995. Does prolonged implantation of depth electrodes predispose the brain to kindling? *Brain Res.* 697 (1–2), 197–204.
- Löscher, W., Hönnack, D., Grämer, M., 1999. Effect of depth electrode implantation with or without subsequent kindling on GABA turnover in various rat brain regions. *Epilepsia Res.* 37 (2), 95–108.
- Marchionni, I., Oberoi, M., Soltesz, I., Alexander, A., 2019. Ripple-related firing of identified deep CA1 pyramidal cells in chronic temporal lobe epilepsy in mice. *Epilepsia Open* 4, 254–263.
- Meisenhelder, S., Quon, R.J., Steimel, S.A., Testorf, M.E., Camp, E.J., Moein, P., Culler 4th, G.W., Gross, R.E., Lega, B.C., Sperling, M.R., Kahana, M.J., Jobst, B.C., 2021. Interictal epileptiform discharges are task dependent and are associated with lasting Electrocorticographic changes. *Cereb Cortex Commun.* 2 (2), tgb019.
- Michalakis, M., Holsinger, D., Ikeda-Douglas, C., Cammisuli, S., Ferbinteanu, J., DeSouza, C., DeSouza, S., Fecteau, J., Racine, R.J., Milgram, N.W., 1998. Development of spontaneous seizures over extended electrical kindling. I. Electrographic, behavioral, and transfer kindling correlates. *Brain Res.* 793 (1–2), 197–211.
- Milgram, N.W., Michael, M., Cammisuli, S., Head, E., Ferbinteanu, J., Reid, C., Murphy, M.P., Racine, R., 1995. Development of spontaneous seizures over extended electrical kindling. II. Persistence of dentate inhibitory suppression. *Brain Res.* 670 (1), 112–120.
- Milikovsky, D.Z., Weissberg, I., Kamintsky, L., Lippmann, K., Schefenbauer, O., Frigerio, F., Rizzi, M., Sheintuch, L., Zelig, D., Ofer, J., Vezzani, A., Friedman, A., 2017. Electrocorticographic dynamics as a novel biomarker in five models of Epileptogenesis. *J. Neurosci.* 37 (17), 4450–4461.
- Mocellin, P., Mikulovic, S., 2021. The role of the medial septum-associated networks in controlling locomotion and motivation to move. *Front Neural Circuits.* 15, 699798.
- Morimoto, K., Mason, S.E., Goddard, G.V., 1987. Kindling-induced changes in the EEG recorded during stimulation from the site of stimulation. II. Comparison between spontaneous and evoked potentials. *Exp. Neurol.* 97 (1), 1–16.
- Mysin, I., Shubina, L., 2023. Hippocampal non-theta state: the “Janus face” of information processing. *Front Neural Circuits.* 17, 1134705.
- Pillai, J., Sperling, M.R., 2006. Interictal EEG and the diagnosis of epilepsy. *Epilepsia* 47 (Suppl. 1), 14–22.
- Pinel, J.P., Rovner, L.I., 1978a. Electrode placement and kindling-induced experimental epilepsy. *Exp. Neurol.* 58 (2), 190–202.
- Pinel, J.P., Rovner, L.I., 1978b. Experimental epileptogenesis: kindling-induced epilepsy in rats. *Exp. Neurol.* 58, 335–346.
- Quon, R.J., Camp, E.J., Meisenhelder, S., Song, Y., Steimel, S.A., Testorf, M.E., Andrew, S., Gross, R.E., Lega, B.C., Sperling, M.R., Kahana, M.J., Jobst, B.C., 2021. Features of intracranial interictal epileptiform discharges associated with memory encoding. *Epilepsia* 62 (11), 2615–2626.
- Racine, R.J., 1972. Modification of seizure activity by electrical stimulation II. motor seizure. *Electroencephalogr. Clin. Neurophysiol.* 32 (3), 281–294.
- Racine, R.J., Mosher, M., Kairiss, E.W., 1988. The role of the pyriform cortex in the generation of interictal spikes in the kindled preparation. *Brain Res.* 454 (1–2), 251–263.
- Reddy, D.S., Mohan, A., 2011. Development and persistence of limbic epileptogenesis are impaired in mice lacking progesterone receptors. *J. Neurosci.* 31 (2), 650–658.
- Reddy, D.S., Rogawski, M.A., 2010. Ganaxolone suppression of behavioral and electrographic seizures in the mouse amygdala kindling model. *Epilepsy Res.* 89 (2–3), 254–260.
- Rusina, E., Bernard, C., Williamson, A., 2021. The Kainic acid models of temporal lobe epilepsy. *eNeuro* 8 (2). ENEURO.0337-20.2021.
- Salami, P., Lévesque, M., Benini, R., Behr, C., Gotman, J., Avoli, M., 2014. Dynamics of interictal spikes and high-frequency oscillations during epileptogenesis in temporal lobe epilepsy. *Neurobiol. Dis.* 67, 97–106.
- Sayin, U., Osting, S., Hagen, J., Rutecki, P., Sutula, T., 2003. Spontaneous seizures and loss of axo-axonic and axo-somatic inhibition induced by repeated brief seizures in kindled rats. *J. Neurosci.* 23 (7), 2759–2768.
- Sheybani, L., Biro, G., Contestabile, A., Seeck, M., Kiss, J.Z., Schaller, K., Michel, C.M., Quairiaux, C., 2018. Electrophysiological evidence for the development of a self-sustained large-scale epileptic network in the kainite mouse model of temporal lobe epilepsy. *J. Neurosci.* 38 (15), 3776–3791.

- Shouse, M.N., King, A., Langer, J., Vreeken, T., King, K., Richkind, M., 1990. The ontogeny of feline temporal lobe epilepsy: kindling a spontaneous seizure disorder in kittens. *Brain Res.* 525, 215–224.
- Sobieszek, A., 1989. Diversity of kindling effects: EEG manifestations in cats during kindling in the hippocampal formation. *Acta Neurobiol. Exp. (Wars)* 49 (6), 337–357.
- Song, H., Tufa, U., Chow, J., Sivanenthiran, N., Cheng, C., Lim, S., Wu, C., Feng, J., Eubanks, J.H., Zhang, L., 2018. Effects of antiepileptic drugs on spontaneous recurrent seizures in a novel model of extended hippocampal kindling in mice. *Front. Pharmacol.* 9, 451.
- Sutula, T.P., Kotloski, R.J., 2017. Kindling: A model and phenomenon of epilepsy. In: Pitkänen, A., Buckmaster, P.S., Galanopoulou, A.S., Moshé, L.S. (Eds.), *Models of Seizures and Epilepsy*, 2nd edition. Academic Press, pp. 813–826.
- Tatum, W.O., Rubboli, G., Kaplan, P.W., Mirsatari, S.M., Radhakrishnan, K., Gloss, D., Caboclo, L.O., Drislane, F.W., Koutroumanidis, M., Schomer, D.L., Kastelein-Nolst Trenite, D., Cook, M., Beniczky, S., 2018. Clinical utility of EEG in diagnosing and monitoring epilepsy in adults. *Clin. Neurophysiol.* 129 (5), 1056–1082.
- Thom, M., Bertram, E.H., 2012. Temporal lobe epilepsy. *Handb. Clin. Neurol.* 107, 225–240.
- Tse, K., Beamer, E., Simpson, D., Beynon, R.J., Sills, G.J., Thippeswamy, T., 2021. The impacts of surgery and intracerebral electrodes in C57BL/6J mouse kainate model of Epileptogenesis: seizure threshold, proteomics, and cytokine profiles. *Front. Neurol.* 12, 625017.
- Ung, H., Cazares, C., Nanivadekar, A., Kini, L., Wagenaar, J., Becker, D., Krieger, A., Lucas, T., Litt, B., Davis, K.A., 2017. Interictal epileptiform activity outside the seizure onset zone impacts cognition. *Brain* 140 (8), 2157–2168.
- Vanderwolf, C.H., 1969. Hippocampal electrical activity and voluntary movement in the rat. *Electroencephalogr. Clin. Neurophysiol.* 26, 407–418.
- Wada, J.A., Osawa, T., 1976. Spontaneous recurrent seizure state induced by daily electric amygdaloid stimulation in Senegalese baboons (*Papio papio*). *Neurology* 26 (3), 273–286.
- Wada, J.A., Sato, M., Corcoran, M.E., 1974. Persistent seizure susceptibility and recurrent spontaneous seizures in kindled cats. *Epilepsia* 15 (4), 465–478.
- Wang, S., Lévesque, M., Avoli, M., 2019. Transition from status epilepticus to interictal spiking in a rodent model of mesial temporal epilepsy. *Epilepsy Res.* 152, 73–76.
- Wauquier, A., Ashton, D., Melis, W., 1979. Behavioral analysis of amygdaloid kindling in beagle dogs and the effects of clonazepam, diazepam, phenobarbital, diphenylhydantoin, and flunarizine on seizure manifestation. *Exp. Neurol.* 64 (3), 579–586.
- White, A., Williams, P.A., Hellier, J.L., Clark, S., Dudek, F.E., Staley, K.J., 2010. EEG spike activity precedes epilepsy after kainate-induced status epilepticus. *Epilepsia* 51 (3), 371–383.
- Wu, C., Wais, M., Sheppy, E., del Campo, M., Zhang, L., 2008. A glue-based, screw-free method for implantation of intra-cranial electrodes in young mice. *J. Neurosci. Methods* 171 (1), 126–131.
- Zahra, A., Sun, Y., Aloysius, N., Zhang, L., 2022. Convulsive behaviors of spontaneous recurrent seizures in a mouse model of extended hippocampal kindling. *Front. Behav. Neurosci.* 16, 1076718.